

STUDYING THE MAIN CHARACTERISTICS OF THE GEMINID METEOR SHOWER FROM BASELINE VIDEO OBSERVATIONS IN 2021

K.I. Ivanov 

Irkutsk State University,
Irkutsk, Russia, ivorypalace@gmail.com

E.S. Komarova

Irkutsk State University,
Irkutsk, Russia, eskomarik@gmail.com

S.A. Yazev

Irkutsk State University,
Irkutsk, Russia, syazev@gmail.com
Institute of Solar-Terrestrial Physics SB RAS,
Irkutsk, Russia

Abstract. The Geminid meteor shower has been studied using data obtained by the method of baseline video observations during the period from December 01, 2021 to December 17, 2021. The meteors were examined in the brightness range from -3^m to 2^m and with an angular track length of at least 2° ; the sample size was 327 events. The behavior of the shower is considered in terms of the interacting DRG (December ρ -Geminids) and GEM (Geminids) branches, which are closely related to each other and share a common origin. The shower activity was $ZHR=127$, $Flux=19$ at the general maximum of DRG+GEM ($\lambda_{sol}\sim 261.8^\circ$) and $ZHR=32$, $Flux=4$ at the putative local maximum of DRG ($\lambda_{sol}\sim 258.8^\circ$). Daily drift values were obtained for GEM ($\Delta\alpha=0.84^\circ$, $\Delta\delta=-0.27^\circ$, $\Delta\lambda_{ec}=0.75^\circ$, $\Delta\beta=-1.17^\circ$) and DRG ($\Delta\alpha=1.29^\circ$, $\Delta\delta=0.09^\circ$, $\Delta\lambda_{ec}=1.09^\circ$, $\Delta\beta=0.23^\circ$) in the equatorial and ecliptic coordinate systems; the

intrinsic drift in the $\lambda_{ec}-\lambda_{sol}$ system was 0.09° and -0.26° for the DRG and GEM components respectively. We have found the opposite nature of the drift of both branches with a tendency for them to intersect at the point $\alpha=112.1^\circ$, $\delta=32.5^\circ$, $\lambda_{sol}=259.8^\circ$. We have determined the kinematic and orbital parameters of meteoroids and have identified differences between the most probable geocentric velocities for the DRG ($v_g=35$ km/s) and GEM ($v_g=34$ km/s) branches. The morphology of the distribution of orbits within the meteor shower has been studied. We give recommendations for reliably determining whether the meteors belong to one or another branch.

Keywords: meteor, meteoroid, meteor shower, Geminids, baseline observations, orbital parameters.

INTRODUCTION

The Geminids are an annual high-intensity meteor shower ($ZHR_{max}\sim 120$) observed in the Northern Hemisphere. They occur on December 7–17, peaking on December 13–14 (the solar longitude in the ecliptic coordinate system $\lambda_{sol}=262.2^\circ$). The radiant point of the shower at maximum is located at $\alpha=112^\circ$, $\delta=+33^\circ$, the daily average drift $\Delta\alpha=+1.04^\circ$, $\Delta\delta=-0.23^\circ$, the average ground speed of meteoroids $v_g\sim 35$ km/s [Jopek et al., 2003] (see the parameters and their designations in Table 3). Annual variations in these parameters are insignificant. The parent body is considered to be asteroid (3200) Phaethon [Hanuš et al., 2016].

The meteor shower is the subject of numerous scientific studies whose relevance is due to the ambiguity in its origin and the presence of a number of features indicating that its structure is nonuniform. In particular, there is a tendency to consider the Geminids as a combination of two separate components (DRG — December ρ -Geminids, GEM — Geminids), which share a common origin and evolve together [Jenniskens et al., 2016; Koseki, 2023]. On the one hand, the presence of a fine structure may suggest that the meteor shower is of cometary origin, as confirmed by numerical simulation methods [Ryabova, 2016, 2021]. On the other hand, differences between kinematic parameters of meteoroids belonging to different parts of the Geminids are insignificant and can be explained in terms of classical concepts provided that the parent body

(3200) Phaethon is considered as an active asteroid [Ryabova, 2012, 2018; Jewitt, 2012]. The third point of view, without denying the importance of the initial conditions and factors [Williams, Ryabova, 2011], assumes that the cause of the occurrence and development of the fine structure of the meteor shower are natural evolutionary processes (gravitational, radiation, erosion). Thus, despite the abundance of experimental data, the problem is far from being solved.

This study may contribute to resolution of existing contradictions. The work is based on experimental data obtained during implementation of the SkyLine project [Ivanov, Komarova, 2016a, b].

1. DATA ACQUISITION AND PROCESSING

The observational material was collected in the Tunka Valley (Republic of Buryatia) from December 01, 2021 to December 17, 2021. Weather conditions at the time were assessed as favorable: minimum clouds and moonlight. The observations were carried out in the basic mode ($d=150$ km), the orientation of the detectors was adjacent-crossed with partial overlap of adjacent regions [Ivanov et al., 2022]. The main observation point is Sayan Solar Observatory of ISTP SB RAS (SSO, $51^\circ 37' 18''$ N, $100^\circ 55' 07''$ E, 2010 m above sea level), the corresponding point is the ISTP SB RAS Geophysical Observatory ($51^\circ 48' 37.5''$ N, $103^\circ 04' 37.4''$ E, 680 m above

sea level) [<https://ru.iszf.irk.ru>]. The meteors were automatically detected by detectors with highly sensitive Watec WAT-910HX CCD video cameras with Smartec STL-3080DC (F0.95.6 mm) lenses forming a video sequence at a resolution of 768×576 pixels at a rate of 25 fr/s. The field of view of each detector is 47°×36° at a scale of 3.75'/pixel, the detectors' total field of view at each point is 5000 deg². The total volume of the detected atmospheric layer in the altitude range 80–120 km exceeds 6 million km³. Efficiency in the basic mode is as high as 55 % of the recorded events.

The events were detected and captured in real time with the software SonotaCo UFOCapture v.2.24 [https://sonotaco.com/soft/e_index.html#ufoa]. Data was stored in AVI format without intermediate compression. The material was primarily selected visually; the main quality criteria were the integrity of the track, the presence of meteor start and end points in the frame, the absence of external noise, and a sufficient number of comparison stars. Astrometric processing of single-sided observations was performed with the software SonotaCo UFOAnalyzer v.4.24 [https://sonotaco.com/soft/e_index.html#ufoa], using the star comparison catalog SKY2000 [<http://td-www.harvard.edu/catalogs/sky2k.html>] in manual mode with constant monitoring of meteor start and end points (criterion $S/N=2$), the photometric light curve, as well as accuracy of meteor path reconstruction. Processing of baseline observations, determination of

orbital parameters, and modeling of space meteoroid trajectories were carried out with the software SonotaCo UFOOrbit v.3.02 [https://sonotaco.com/soft/e_index.html#ufoa].

The processing results were additionally selected according to the criteria given in Table 1. We have chosen 327 events reliably associated with the Geminid meteor shower. Averaged errors in calculating the parameter are shown in Table 2.

2. RESEARCH AND RESULTS

To visually assess the activity of meteor showers, the ZHR (Zenith Hour Rate) parameter is traditionally used [Brown, 1990], which characterizes the number of meteors brighter than +6.5^m when the radiant point is at the zenith. We also employ the Incident Flux Density (*Flux*) [Molau et al., 2014], i.e. the number of meteors brighter than +6.5^m per unit area of the atmosphere per unit time. Activity of the Geminid meteor shower was evaluated according to both criteria by the method detailed in [Vida et al., 2022; Koschack, Rendtel, 1990a, b], taking into account the specifics of the hardware and software in use. The observational results from SSO were utilized as initial data. To ensure maximum accuracy of the analysis, we excluded the events recorded during partial clouds from the sample. The results are presented in Figure 1.

Table 1

Criteria for selecting the results of preprocessing for subsequent analysis

Parameter	Value
The number of reference stars n	≥ 10
Meteor peak magnitude m_{\max}	$-3^m \leq m \leq 2^m$
Error in finding an arbitrary trajectory point (α, δ)	$\pm 0.1^\circ$
Error in determining the radiant point (α, δ)	$\pm 0.1^\circ$
Time synchronization error Δt	± 0.5 s
Angular track length l	$\geq 2^\circ$
Deviation of the ground speed from the catalog Δv_g	± 10 %
Heliocentric speed v_h	> 12 km/s
Orbital eccentricity e	< 1
Internal parameter of UFOOrbit quality assessment [Vereš, Toth, 2010]	> 0.7

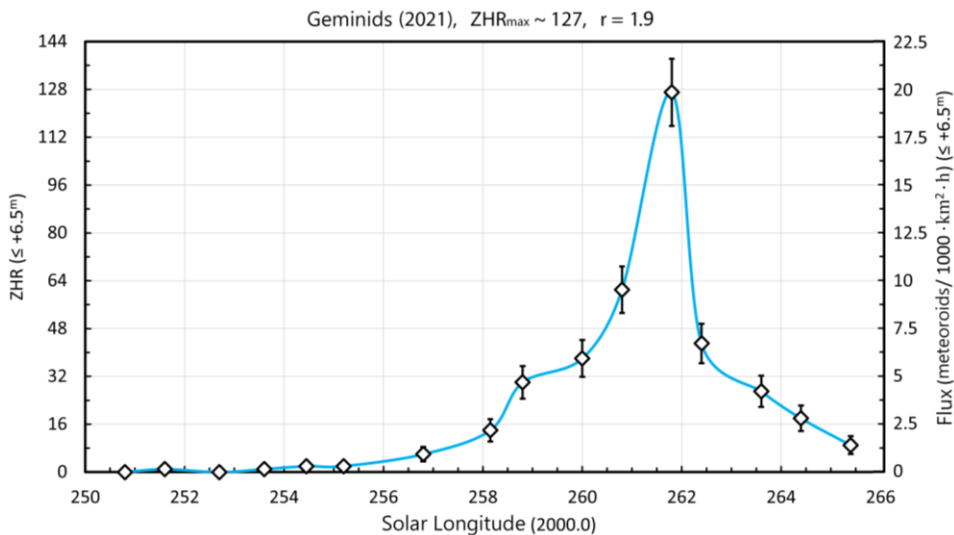


Figure 1. Geminid meteor shower activity (2021)

The meteor shower peaked at $\lambda_{\text{sol}} \sim 261.8^\circ$ (the night of December 13–14). Maximum *Flux* and *ZHR* were 19 and 127 respectively, which is typical of the Geminids and is consistent with reference data [<https://www.ta3.sk/IAUC22DB/MDC2022/Etc/streamfulldata2022.txt>] and the results of other research teams [Vida et al., 2022; https://www.imon.net/members/imo_live_shower/summary?shower=QUA&year=2021]. Throughout the observation period, the meteor shower demonstrated typical dynamics characterized by a pronounced, well-localized peak near the time of GEM maximum ($\lambda_{\text{sol}} \sim 261.8^\circ$), as well as a smooth increase and decrease around it. A slight asymmetry of the profile to the left of the maximum near $\lambda_{\text{sol}} \sim 258.8^\circ$ may indicate a burst of activity of DRG (December ρ -Geminids) that is part of the Phaethon complex and is probably closely related to the main meteor shower. The measured activity of the meteor shower at the time of the estimated local DRG maximum was *ZHR*=32 and *Flux*=4. The observations were ceased on December 17, 2021 due to adverse weather conditions. There were no abnormal upward or downward changes in the meteor shower activity.

Kinematic characteristics of the meteoroids were analyzed based on the results of data processing. The frequen-

cy distribution of ground and heliocentric meteoroid speeds was analyzed separately for the DRG and GEM components of the stream in comparison with the mathematical model — the Gaussian function normalized to the maximum number of meteoroids in the velocity range in increments of 1 km/s:

$$\varphi(v) = \frac{1}{\sigma\sqrt{2\pi}} e^{-(v-a)^2/2\sigma^2}. \quad (1)$$

Here, a and σ are the mathematical expectation and the standard deviation respectively, calculated individually for each sample:

$$a(v) = \sum_{i=1}^n v_i p_i, \quad (2)$$

$$\sigma = \sqrt{D(v)}, \quad (3)$$

$$D(v) = \sum_{i=1}^n (v_i - a)^2 p_i, \quad (4)$$

where p_i is the probability of finding a value from $v_i - v_{i+1}$ in the total sample. The frequency distribution of the calculated speeds in increments of 1 km/s is illustrated in Figure 2.

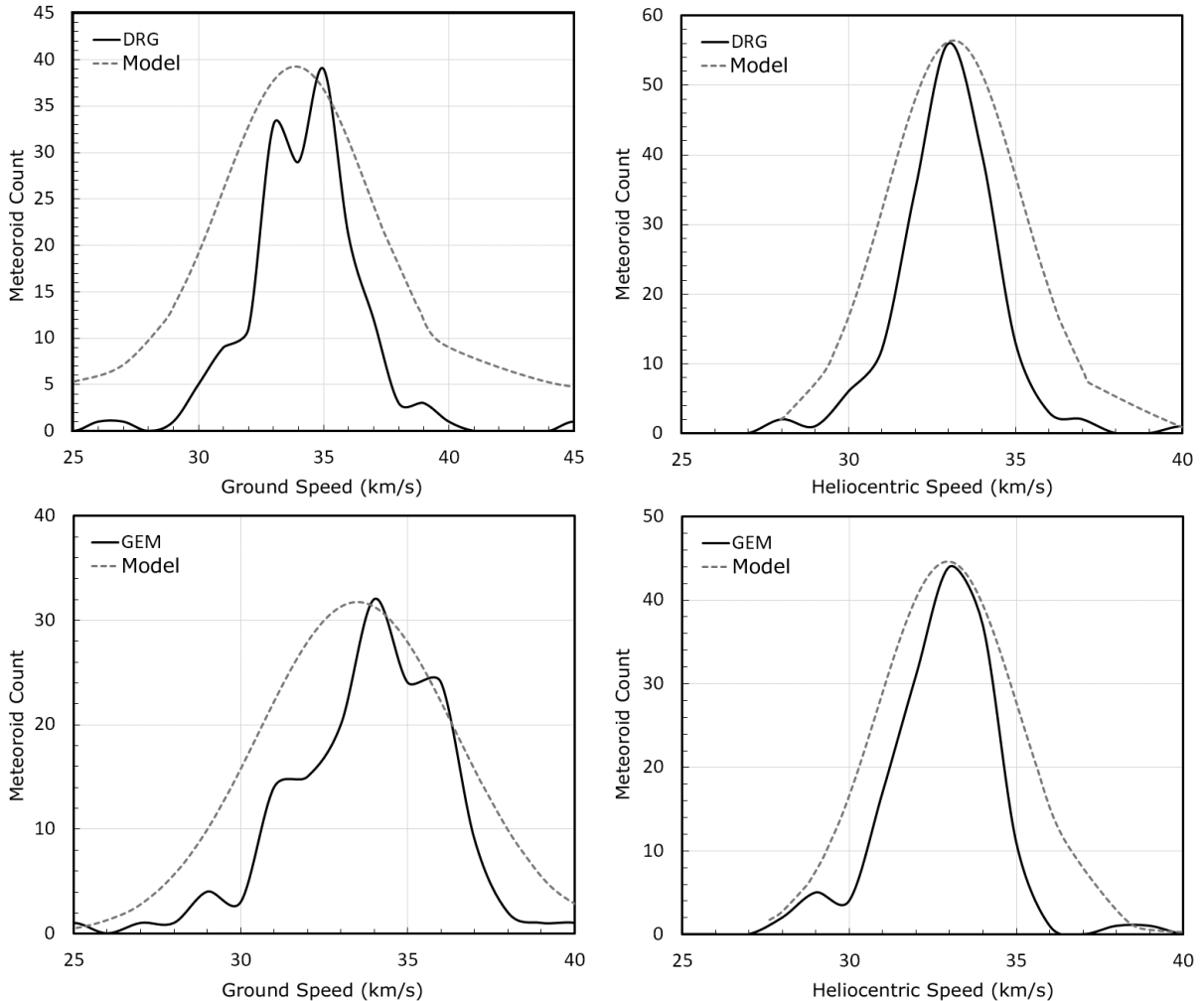


Figure 2. Frequency distribution of speeds of DRG and GEM meteor shower components (2021) in comparison with the mathematical model of normal distribution

The measured heliocentric speeds v_h of meteoroids of both Geminid components demonstrate a sufficiently high degree of correspondence with the mathematical model and a pronounced symmetry of the profile, which suggests that dispersion of the kinematic parameters of meteoroids in the stream in this portion of the orbit is uniform. The most common heliocentric speeds of DRG and GEM are ~ 33 km/s and show no significant difference within the sample under study. On the contrary, ground speeds v_g of both meteor stream components are unstable, which may be due to the peculiarities of observations (mainly in the evening and morning due to the need to select data according to meteorological conditions), measurement errors, and small sample size. The most probable speed for GEM meteoroids $v_g \sim 34$ km/s corresponds to the reference data, whereas for DRG meteoroids it is slightly higher on average, ~ 35 km/s.

Drift parameters were calculated in a linear approximation by the least square method separately for DRG and GEM; the results are presented in Figure 3. We found a pronounced drift of both components toward each other along each axis, which can be explained by the peculiarities of the meteor shower pattern.

Along with the daily drift, the components demonstrate the intrinsic drift not caused by the orbital motion of Earth: 0.09° and -0.26° for DRG and GEM respectively in the coordinate system $\lambda_{ec}-\lambda_{sol}$. Both components have almost simultaneous activity peak near $\lambda_{sol} \sim 261.8^\circ$, whereas their intersection point is located near the peak, but does not coincide with it ($\lambda_{sol} \sim 259.9^\circ$), which can also be attributed

to the peculiarities of the meteor shower pattern and distribution. The relative location of the DRG and GEM radiation areas as a function of equatorial coordinates and solar longitude is depicted in Figure 4. The radius of the areas corresponds to $3\sigma_{aver}$ (see Table 2). Information on the drift parameters is given in Table 3.

Figure 5 illustrates the distribution of individual radiant points in the equatorial and ecliptic coordinate systems after reduction to the time of maximum ($\lambda_{sol} \sim 261.8^\circ$).

The DRG and GEM components form a single radiation area with a fairly noticeable separation between impact areas, which may be indirect evidence of the stream anisotropy in this portion of the orbit. It should, however, be taken into account that the radiant points are very close, especially near the maximum, that is why some meteors when processed might have been assigned to the wrong component. In general, the stream features a high density and relative uniformity of distribution in the center of the meteoroid stream and an increase in dispersion and anisotropy to the periphery. The latter can be caused both by natural physical processes accompanying the evolution of the meteoroid stream and by random fluctuations in parameters against the background of the small sample. In any case, the stream is characterized by a fairly compact radiation area whose estimated dimensions are $\Delta\alpha=6.12^\circ$, $\Delta\delta=4.98^\circ$; $\Delta\lambda_{ec}=5.67^\circ$, $\Delta\beta=5.71^\circ$. Calculated equatorial coordinates of the radiant center are $\alpha=113.52^\circ$, $\delta=32.48^\circ$.

Table 2

 Averaged errors in calculating parameter values
for the analyzed sample of Geminid meteoroids

Parameter	GEM+DRG		GEM		DRG	
	$\pm\Delta x_{ave}$ r	σ_{aver}	$\pm\Delta x_{av}$ er	σ_{aver}	$\pm\Delta x_{av}$ er	σ_{aver}
Right ascension $\alpha(RA)$, $^\circ$	0.24	0.60	0.26	0.67	0.21	0.52
Declination $\delta(Dec)$, $^\circ$	0.23	0.58	0.28	0.70	0.18	0.47
Solar longitude λ_{sol} , $^\circ$	0.24	0.57	0.25	0.65	0.20	0.49
Ecliptic longitude λ_{ec} , $^\circ$	0.22	0.54	0.24	0.61	0.19	0.51
Ecliptic latitude β , $^\circ$	0.23	0.57	0.25	0.63	0.21	0.56
Ground speed v_g , km/s	0.54	1.38	0.66	1.65	0.42	1.08
Heliocentric speed v_h , km/s	0.40	1.02	0.43	1.07	0.37	0.93
Semi-major axis a , AU.	0.13	0.33	0.11	0.28	0.15	0.38
Perihelion distance q , AU.	0.026	0.067	0.021	0.052	0.031	0.077
Orbital eccentricity e	0.033	0.083	0.028	0.069	0.038	0.095
Orbital period p , years	0.11	0.27	0.09	0.23	0.12	0.32
Argument of perihelion Π , $^\circ$	0.20	0.51	0.14	0.35	0.26	0.67
Longitude of ascending node Ω , $^\circ$	0.24	0.62	0.17	0.43	0.31	0.82
Orbital inclination i , $^\circ$	0.51	1.24	0.33	0.83	0.67	1.72

Table 3

Calculated parameters of daily drift of the GEM and DRG components

	$\Delta\alpha$, $^\circ$	$\Delta\delta$, $^\circ$	$\Delta\lambda_{ec}$, $^\circ$	$\Delta\beta$, $^\circ$	$\Delta(\lambda_{ec}-\lambda_{sol})$, $^\circ$
GEM	+0.84	-0.27	+0.75	-1.17	-0.26
DRG	+1.29	+0.09	+1.09	+0.23	+0.09

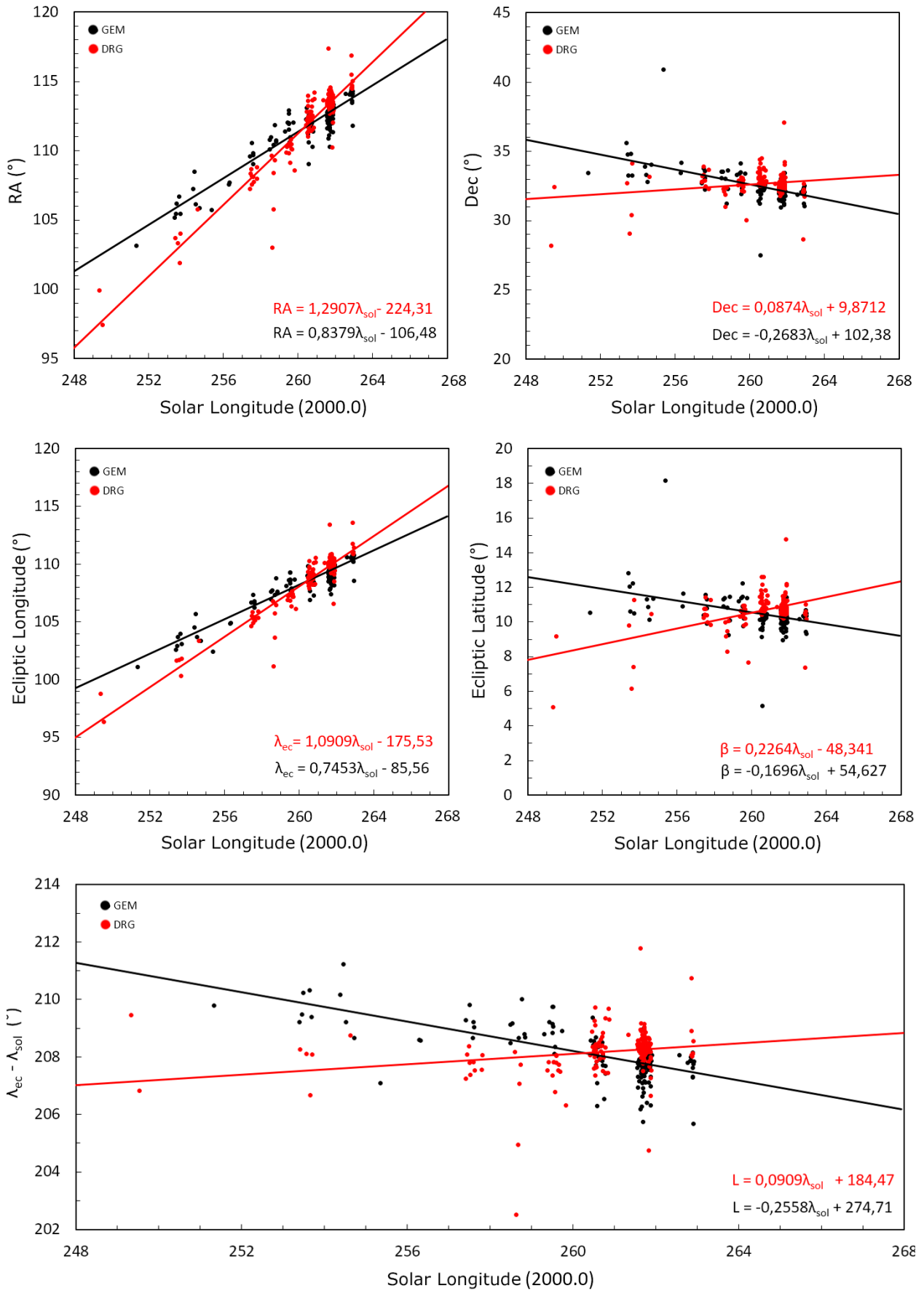


Figure 3. Drift parameters of the DRG and GEM meteor stream components (2021)

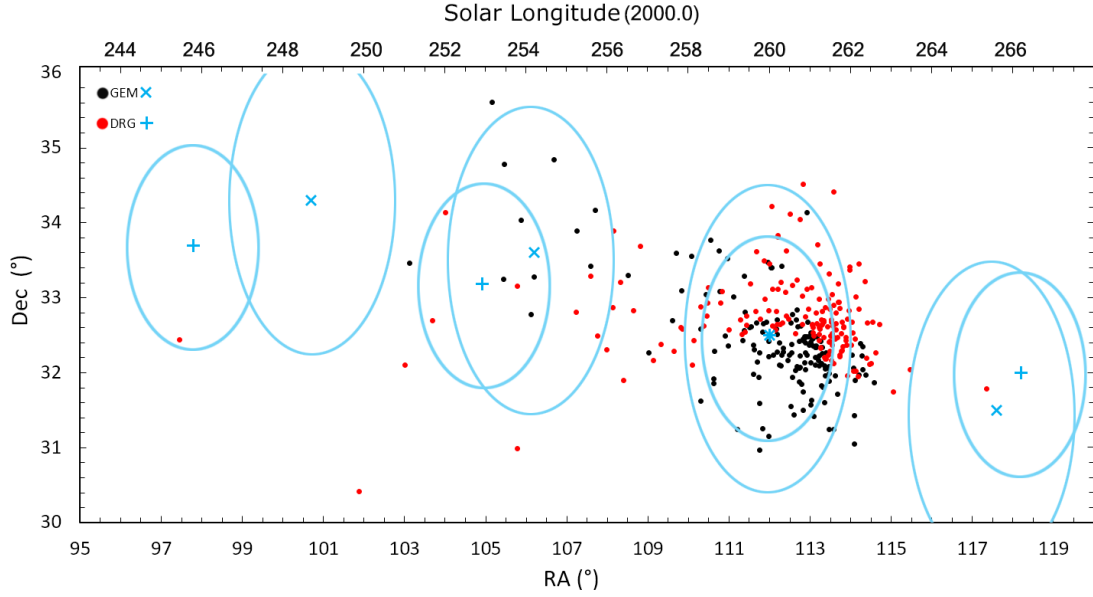


Figure 4. Intrinsic drift of radiation areas of the DRG and GEM meteor stream components (2021). Calculated point of intersection of radiants: $\alpha=112.1^\circ$, $\delta=32.5^\circ$, $\lambda_{\text{sol}}=259.8^\circ$

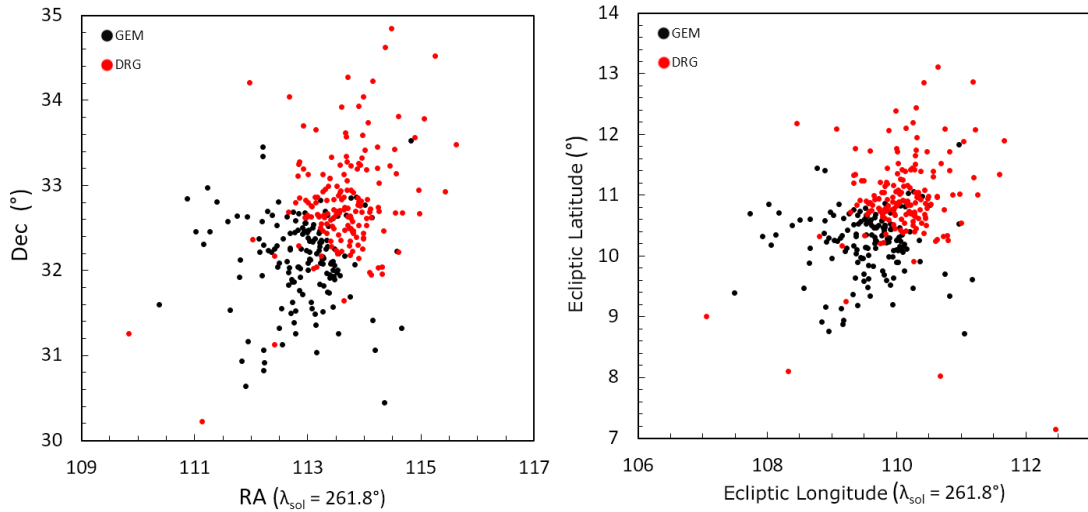


Figure 5. Distribution of radiant points of the DRG and GEM meteor stream components (2021) minus daily drift

The daily drift along the axes of right ascension, declination, ecliptic longitude and latitude is for DRG $\Delta\alpha=1.29^\circ$, $\Delta\delta=0.09^\circ$, $\Delta\lambda_{\text{ec}}=1.09^\circ$, $\Delta\beta=0.23^\circ$, and for GEM

$$\Delta\alpha=0.84^\circ, \Delta\delta=-0.27^\circ, \Delta\lambda_{\text{ec}}=0.75^\circ, \Delta\beta=-1.17^\circ.$$

The results of calculations of inclination and arguments of perapsis for DRG and GEM are presented in Figure 6. The relation between these parameters characterizes meteoroid distribution in the cross-section of the meteoroid stream near perihelion, which appears to be quite compact, isotropic, and uniform. Both parts of the stream exhibit uniform scattering around the center and a commensurate contribution to the overall picture. Dispersion increases expectedly from the center to the periphery with a slight tendency for the argument of perapsis and inclination to decrease, which may result from natural evolutionary processes. The meteor shower does not show pronounced bunches and branches.

Distribution of the ratios of the semi-major axis to the perihelion distance for both components (Figure 6) is quite dense, which indicates a high degree of compact-

ness of the meteor shower. DRG and GEM make a commensurate contribution to the overall pattern of meteoroid distribution and are localized in an area centered at $q=0.15$ AU, $a=1.24$ AU, which with high accuracy corresponds to similar parameters of the assumed parent body ((3200) Phaeton: $q=0.14$ AU, $a=1.27$ AU) and may indicate a relatively young age of the stream and/or minor external influence on its evolution. A notable feature of DRG is the presence of meteoroids with more elongated orbits at a sufficiently small perihelion distance: apparently, this factor determines their higher velocity, which, along with an earlier time of maximum, gives reason to consider DRG as a separate structural element.

Dependence of the main orbital parameters on the solar longitude is shown in Figure 7. DRG and GEM exhibit a symmetrical counter trend of the perihelion distance with

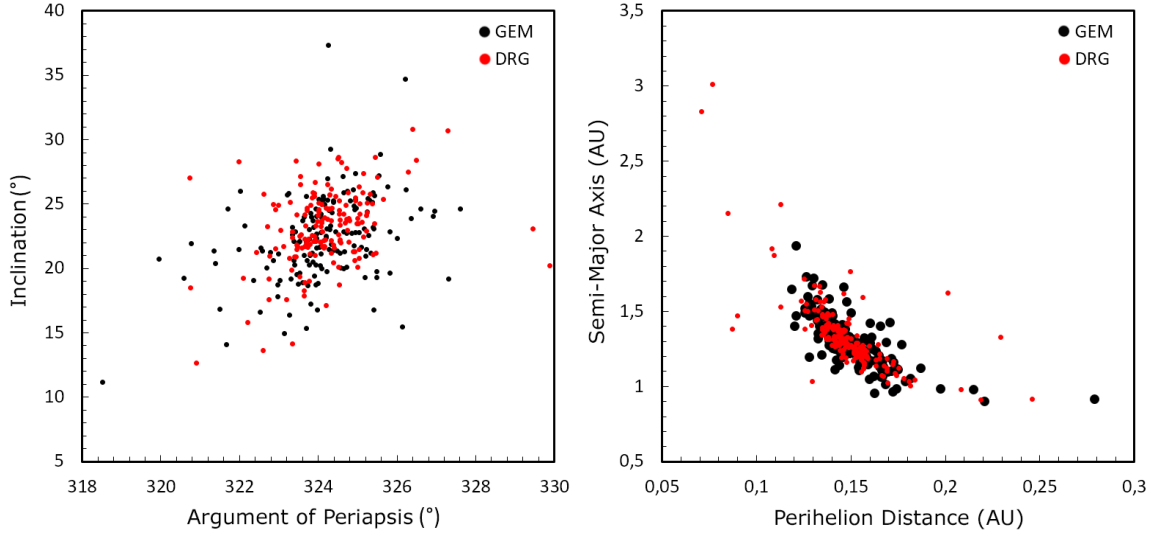


Figure 6. Structure of the Geminid meteor shower (2021) near perihelion

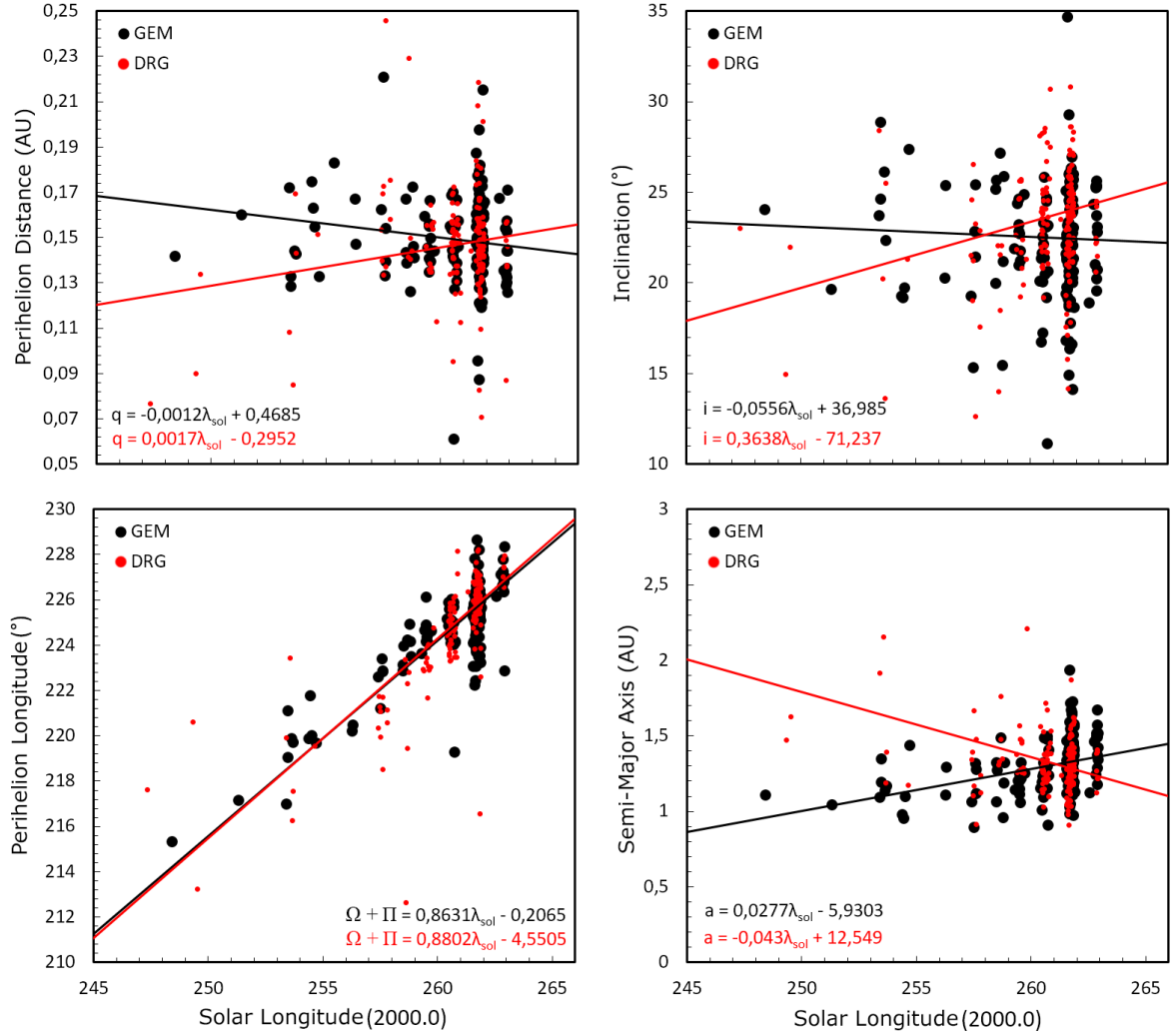


Figure 7. Main orbital parameters of the DRG and GEM meteor stream components (2021) as a function of solar longitude

an intersection point near the maximum, with the meteor shower as a whole having a stable value of $q \sim 0.15$ AU throughout the observation period. This behavior can be explained both by the mechanics of the shower itself and by the probable cross-identification of meteors

due to the proximity of radiation areas. More accurate identification of the cause of the observed effect requires follow-up studies based on a larger sample.

Similar conclusions are also valid for orbital inclinations. The meteor stream components exhibit similar

behavior and a counter trend, yet for the meteor shower as a whole the trend turns out to be positive and is $\sim 0.16^\circ/\text{day}$, whereas the averaged inclination of the meteor shower is always $\sim 22^\circ$ and corresponds to that of the parent body. Variance of the parameter increases over time to 20° at maximum.

The perihelion longitudes of DRG and GEM demonstrate an almost synchronous upward trend and a small level of dispersion (about 7°), which allows us to consider the meteor shower as a whole. The semi-major orbital axis despite the counter trend of individual components remains almost constant for the meteor shower as a whole and is ~ 1.3 AU (at $a = 1.27$ AU for the parent body). The measured variance of this parameter does not exceed 1 AU and has no pronounced time dependence.

The set of individual orbits of Geminid meteoroids is shown in Figure 8. Figure 8 indicates that the meteoroid stream near perihelion has a very dense structure and compact dimensions; a similar situation with a slightly larger dispersion persists when the stream approaches Earth (see projections A and C). All orbits of the meteoroids included in the sample lie within Jupiter's orbit.

The meteor shower visually retains relative isotropy and uniformity in all orbital portions; however, it reveals a pronounced tendency to increase the semi-major axes of the meteoroids as orbital inclination, presumably caused by natural evolutionary processes, increases (Figure 8, projection B). Referring to Figure 9, a significant number of the meteoroids of both parts of the stream is evenly distributed within a relatively compact region, with DRG meteoroids having generally higher orbital inclinations than GEM ones. There is an obvious positive trend in orbital inclination of both components

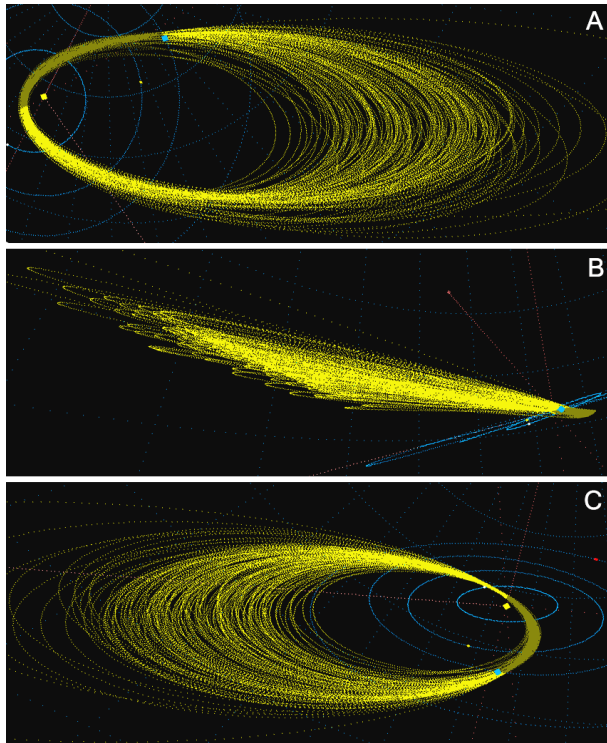


Figure 8. Individual orbits of Geminid meteoroids (2021) from the results of observational data analysis

with an increase in semi-major axes, yet the approximated increase in the orbital inclination for DRG is somewhat lower due to the values comprising an almost uniform series below the main area. The stable nature of the series and the membership of all values to DRG suggest its natural origin, but the effect of measurement errors cannot be excluded.

3. DISCUSSION AND CONCLUSIONS

The available observational data indicate the bimodality of the *ZHR* and *Flux* profiles of the Geminid meteor shower. A burst of activity near $\lambda_{\text{sol}} \sim 258.8^\circ$ is presumably characteristic of the DRG component and can be considered as an additional argument for the existence of a separate structural element. Another important feature of DRG observed by research teams is higher ground speeds of meteoroids — to 40 km/s versus 35 km/s for GEM [Jenniskens et al., 2016]. While in this work the difference between ground speeds of DRG and GEM did not exceed 1 km/s, it is reasonable to take into account this feature in the operational differentiation of the components, which is not inferior in importance to generally accepted criteria based on determining coordinates of individual radiant points and predicted times of maximum [Neslušan, Hajdukova, 2017; Jopek et al., 1999]. This is especially significant due to the proximity of the DRG and GEM radiant points, minor differences between orbital parameters of the meteoroids included in them, as well as the presence of features indicating counter motion of the components with a tendency to intersect near GEM peak. Note that these features and unavoidable measurement and calculation errors can lead to erroneous assignment of meteors to one or another part of the stream. Follow-up studies are required in order to confirm or refute the effects.

Since the morphological structure of the Geminid meteor shower appears to be quite uniform (especially near perihelion) and does not have pronounced features, even taking into account the signs of the presence of the two overlapping components DRG and GEM, we do not yet have sufficient grounds to state that they are of different origins. Taking into account the very similar characteristics of meteoroids, it is most advisable to consider DRG as a structural element of the main GEM meteor shower formed during natural evolutionary processes, or an indirect sign of activity of parent asteroid (3200) Phaethon [Licandro et al., 2007]. The assumption about the presence of a separate parent body, put forward by some authors as an alternative hypothesis for the origin of the GEM components [Ohtsuka et al., 2006], has not been confirmed in this work.

In the study, we have obtained independent data on the main parameters of the Geminid meteor shower, which do not contradict the already known ones and clarify them. Meteor shower activity near maximum ($\lambda_{\text{sol}} \sim 261.8^\circ$) was $ZHR=127$, $Flux=19$; the contribution of DRG and GEM is estimated as commensurate. The daily drift in the equatorial and ecliptic coordinate systems is $\Delta\alpha=0.84^\circ$, $\Delta\delta=-0.27^\circ$, $\Delta\lambda_{\text{ec}}=0.75^\circ$, $\Delta\beta=-1.17^\circ$ for GEM and $\Delta\alpha=1.29^\circ$, $\Delta\delta=0.09^\circ$, $\Delta\lambda_{\text{ec}}=1.09^\circ$, $\Delta\beta=0.23^\circ$ for DRG; the intrinsic drift in the $\lambda_{\text{ec}}-\lambda_{\text{sol}}$ system is 0.09° and -0.26° for DRG and GEM

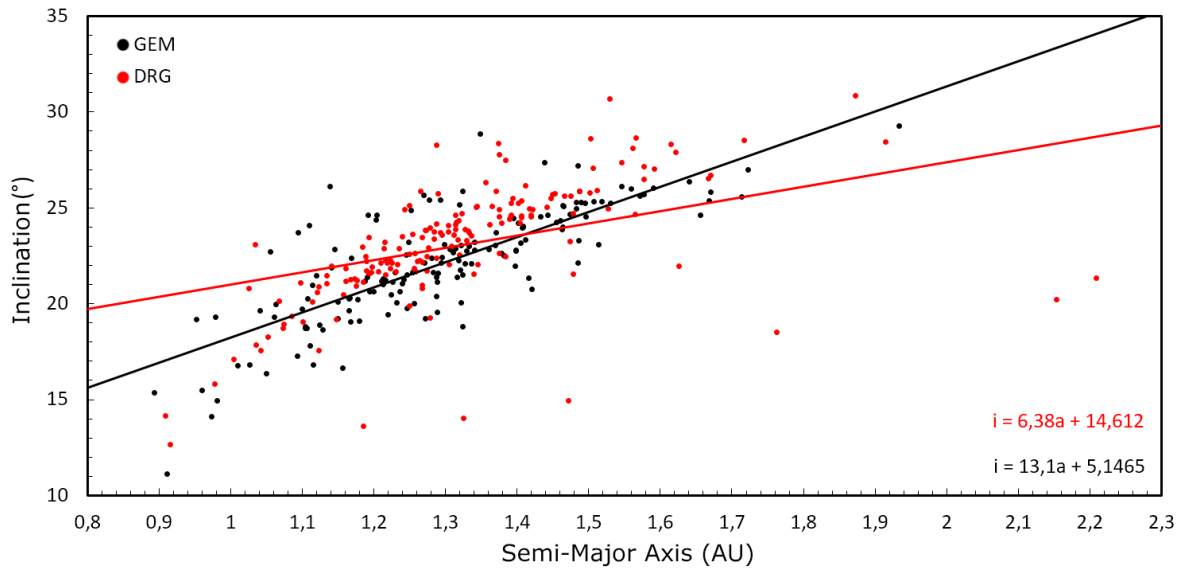


Figure 9. Orbital inclinations of DRG and GEM meteoroids (2021) as a function of semi-major axes

respectively. We have also obtained data indicating a counter drift of both parts intersecting at $\alpha=112.1^\circ$, $\delta=32.5^\circ$, $\lambda_{\text{sol}}=259.8^\circ$. A similar tendency is observed for some orbital parameters such as perihelion distance ($\Delta q_{\text{GEM}}=-0.0012$ AU, $\Delta q_{\text{DRG}}=+0.0017$ AU), inclination ($\Delta i_{\text{GEM}}=-0.056^\circ$, $\Delta i_{\text{DRG}}=+0.0364^\circ$), and semi-major axis ($\Delta a_{\text{GEM}}=+0.028$ AU, $\Delta a_{\text{DRG}}=-0.043$ AU). At the same time, drift of the perihelion longitude for both components is co-directional and almost synchronous ($\Delta \Omega_{\text{GEM}}+\Pi_{\text{GEM}}=+0.86^\circ$, $\Delta \Omega_{\text{DRG}}+\Pi_{\text{DRG}}=+0.88^\circ$), minor differences may be due to the measurement error. The dependence $i(a)$, on the contrary, has a counter trend, is pronounced, and amounts to $\Delta i_{\text{GEM}}=+6.38^\circ$, $\Delta i_{\text{DRG}}=+13.10^\circ$.

The described features of the behavior of DRG and GEM may be an objective consequence of the processes accompanying the evolution of the meteoroid stream; it is, however, necessary to take into account the possibility of cross-identification of events due to very similar characteristics of meteoroids of both components.

The work was performed with Unique Research Facility "Astrophysical Complex" and was financially supported by the Ministry of Science and Higher Education of the Russian Federation (Agreement EB-075-15-2021-675, Government assignment FZZE-2020-0024, FZZE-202-0004).

REFERENCES

- Brown P. On the cause and nature of error in zenithal hourly rates. *WGN, Journal of the IMO*. 1990, vol. 18, pp. 141–145.
- Hanuš J., Delbo M., Vokrouhlický D., Pravec P., Emery J.P., Alí-Lagoa V., Bolin B., Devogèle M., et al. Near-Earth asteroid (3200) Phaethon: Characterization of its orbit, spin state, and thermophysical parameters. *Astron. Astrophys.* 2016, vol. 592, no. A34. DOI: [10.1051/0004-6361/201628666](https://doi.org/10.1051/0004-6361/201628666).
- Ivanov K.I., Komarova E.S. SkyLine project – a new stage in the development of meteor astronomy in Pribaikalye. *Izbrannye problemy astronomii [Selected problems of astronomy: Proc. IV All-Russian Astronomical Conference "Sky and Earth", dedicated to the 85th anniversary of the astronomical observatory of ISU]*. 2016a, pp. 76–83. (In Russian).
- Ivanov K.I., Komarova E.S. SkyLine is a universal project of meteors video surveillance. *Izvestiya Irkutskogo gosudarstvennogo universiteta. Seriya "Nauki o Zemle" [The Bulletin of Irkutsk State University. Series "Earth Sciences"]*. 2016b, vol. 16, pp. 55–66. (In Russian).
- Ivanov K.I., Komarova E.S., Yazev S.A. A comprehensive study of the Perseid stream bolide using the data of the Sky-Line baseline video monitoring system. *Astronomy Reports*. 2022, vol. 66, iss. 6, pp. 513–520. DOI: [10.1134/S1063772922070034](https://doi.org/10.1134/S1063772922070034).
- Jenniskens P., Nénon Q., Albers J., Gural P.S., Haberman B., Holman D., Morales R., Grigsby B.J., Samuels D., Johannink C. The established meteor showers as observed by CAMS. *Icarus*. 2016, vol. 266, pp. 331–354. DOI: [10.1016/j.icarus.2015.09.013](https://doi.org/10.1016/j.icarus.2015.09.013).
- Jewitt D. The active asteroids. *Astron. J.* 2012, vol. 143, no. 3, pp. 66–80. DOI: [10.2458/azu_uapress_9780816532131-ch012](https://doi.org/10.2458/azu_uapress_9780816532131-ch012).
- Jopek T.J., Valsecchi G.B., Froeschle C.I. Meteoroid stream identification: a new approach – II. Application to 865 photographic meteor orbits. *Mont. Not. Roy. Astron. Soc.* 1999, vol. 304, pp. 751–758. DOI: [10.1046/j.1365-8711.1999.02265.x](https://doi.org/10.1046/j.1365-8711.1999.02265.x).
- Jopek T.J., Valsecchi G.B., Froeschlé C.I. Meteor stream identification: a new approach – III. The limitations of statistic. *Mont. Not. Roy. Astron. Soc.* 2003. Vol. 344. P. 665–672. DOI: [10.1046/j.1365-8711.2003.06888.x](https://doi.org/10.1046/j.1365-8711.2003.06888.x).
- Koschack R., Rendtel J. Determination of spatial number density and mass index from visual meteor observations (I). *WGN, J. IMO*. 1990a, vol. 18-2, pp. 44–58.
- Koschack R., Rendtel J. Determination of spatial number density and mass index from visual meteor observations (I). *WGN, J. IMO*. 1990b, vol. 18-4, pp. 119–140.
- Koseki M. Major meteor showers based on Global Meteor Network data. *eMetN Meteor J.* 2023, vol. 8, no. 4, pp. 231–245.
- Licandro J., Campins H., Mothé-Diniz T., Pinilla-Alonso N., de León J. The nature of comet-asteroid transition object (3200) Phaethon. *Astron. Astrophys.* 2007, vol. 461, no. 2, pp. 751–757. DOI: [10.1051/0004-6361:20065833](https://doi.org/10.1051/0004-6361:20065833).
- Molau S., Barentsen G., Crivello S. Obtaining population indices from video observations of meteors. *Proc. of the IMC*. 2014, pp. 74–80.
- Neslušán L., Hajduková M. Separation and confirmation of showers. *Astron. Astrophys.* 2017, vol. 598. DOI: [10.1051/0004-6361/201629659](https://doi.org/10.1051/0004-6361/201629659).
- Ohtsuka K., Sekiguchi T., Kinoshita D., Watanabe J.-I., Ito T., Arakida H., Kasuga T. Apollo asteroid 2005 UD: split

nucleus of (3200) Phaethon? *Astron. Astrophys.* 2006, vol. 450, pp. L25–L28. DOI: [10.1051/0004-6361:200600022](https://doi.org/10.1051/0004-6361:200600022).

Ryabova G.O. On the possible ejection of meteoroids from asteroid (3200) Phaethon in 2009. *Mont. Not. Roy. Astron. Soc.* 2012, vol. 423, iss. 3, pp. 2254–2259. DOI: [10.1111/j.1365-2966.2012.21033.x](https://doi.org/10.1111/j.1365-2966.2012.21033.x).

Ryabova G.O. A preliminary numerical model of the Geminid meteoroid stream. *Mont. Not. Roy. Astron. Soc.* 2016, vol. 456, iss. 1, pp. 78–84. DOI: [10.1093/mnras/stv2626](https://doi.org/10.1093/mnras/stv2626).

Ryabova G.O. Could the Geminid meteoroid stream be the result of long-term thermal fracture? *Mont. Not. Roy. Astron. Soc.* 2018, vol. 479, iss. 1, pp. 1017–1020. DOI: [10.1093/mnras/sty1532](https://doi.org/10.1093/mnras/sty1532).

Ryabova G.O. The Geminid meteor shower radiant: a mathematical model. *Mont. Not. Roy. Astron. Soc.* 2021, vol. 507, iss. 1, pp. 4481–4486. DOI: [10.1093/mnras/stab2286](https://doi.org/10.1093/mnras/stab2286).

Vereš P., Toth J. Analysis of the SonotaCo video meteoroid orbits. *WGN, Journal of the IMO.* 2010, vol. 38, no. 2, pp. 54–57.

Vida D., Blaauw E., Brown P., Kambulow J., Campbell-Brown M., Mazur M.J. Computing optical meteor flux using Global Meteor Network data. *Mont. Not. Roy. Astron. Soc.* 2022, vol. 515, iss. 2, pp. 2322–2339. DOI: [10.1093/mnras/stac1766](https://doi.org/10.1093/mnras/stac1766).

Williams I.P., Ryabova G.O. Meteor shower features: are they governed by the initial formation process or by subsequent gravitational perturbations? *Mont. Not. Roy. Astron. Soc.* 2011, vol. 415, iss. 4, pp. 3914–3920. DOI: [10.1111/j.1365-2966.2011.19010.x](https://doi.org/10.1111/j.1365-2966.2011.19010.x).

URL: <http://tdc-www.harvard.edu/catalogs/sky2k.html> (accessed September 2, 2024).

URL: https://ru.iszf.irk.ru/Generic_page (accessed September 2, 2024).

URL: https://sonotaco.com/soft/e_index.html#ufoa (accessed September 2, 2024).

URL: <https://www.ta3.sk/IAUC22DB/MDC2022/Etc/stre-amfulldata2022.txt> (accessed September 2, 2024).

URL: https://www.imo.net/members/imo_live_shower?shower=GM&year=2021 (accessed September 2, 2024)

Original Russian version: Ivanov K.I., Komarova E.S., Yazev S.A., published in *Solnechno-zemnaya fizika*. 2024. Vol. 10. No. 4. P. 122–131. DOI: [10.12737/szf-104202413](https://doi.org/10.12737/szf-104202413). © 2024 INFRA-M Academic Publishing House (Nauchno-Izdatelskii Tsentr INFRA-M)

How to cite this article

Ivanov K.I., Komarova E.S., Yazev S.A. Studying the main characteristics of the Geminid meteor shower from baseline video observations in 2021. *Solar-Terrestrial Physics*. 2024. Vol. 10. Iss. 4. P. 114–123. DOI: [10.12737/stp-104202413](https://doi.org/10.12737/stp-104202413).